

Article

Effective Production of 5-Hydroxymethylfurfural from Fructose over a Highly Active Sulfonic Acid Functionalized SBA-15 Catalyst

Yutong Zhu ¹, Ke Song ^{1,2,*}, Xiaofei Xu ¹, Jian He ^{1,2} and Jie Guo ^{1,2} 

¹ Key Laboratory of Hunan Forest Products and Chemical Industry Engineering, Jishou University, Zhangjiajie 427000, China

² College of Chemistry and Chemical Engineering, Jishou University, Jishou 416000, China

* Correspondence: kesong@jsu.edu.cn

Abstract: Utilizing sugar compounds (such as fructose) as feedstock for conversion to HMF is very appealing, because it makes the production processes sustainable and improves the economic viability of platform molecules derived from biomass. Here, SBA-15 with sulfonic acid functionalization was created as a heterogeneous base catalyst for fructose hydrolysis reactions to create significant platform chemicals. A fructose conversion rate as high as 100%, along with a 78.7% yield of HMF, were obtained in DMSO at 130 °C after 1 h. The excellent catalytic performance of SBA-15-SO₃H in fructose hydrolysis reactions was confirmed by the activation energy's low value (56.99 kJ/mol). The mild conditions, fast rate of reaction, and simple operation are worth mentioning for other catalysts. SBA-15-SO₃H has the potential to promote fructose conversion at lower temperatures.

Keywords: 5-hydroxymethylfurfural; fructose dehydration; SBA-15; sulfonic acid functionalized; kinetic study



Citation: Zhu, Y.; Song, K.; Xu, X.; He, J.; Guo, J. Effective Production of 5-Hydroxymethylfurfural from Fructose over a Highly Active Sulfonic Acid Functionalized SBA-15 Catalyst. *Catalysts* **2022**, *12*, 984. <https://doi.org/10.3390/catal12090984>

Academic Editors: Leichang Cao and Hu Li

Received: 25 July 2022

Accepted: 29 August 2022

Published: 31 August 2022

Publisher's Note: MDPI stays neutral with regard to jurisdictional claims in published maps and institutional affiliations.



Copyright: © 2022 by the authors. Licensee MDPI, Basel, Switzerland. This article is an open access article distributed under the terms and conditions of the Creative Commons Attribution (CC BY) license (<https://creativecommons.org/licenses/by/4.0/>).

1. Introduction

The chemical industry is searching to develop biobased alternatives to petroleum-based platform compounds to reduce dependence on nonrenewable fossil resources and decrease greenhouse gas emissions [1]. Biomass, a renewable carbon resource, is being developed to produce liquid fuels as a sustainable alternative to fossil energy. One of the most important biomass resources is carbohydrates, which can be dehydrated to 5-hydroxymethylfurfural (HMF) through the acid-catalyzed process. HMF has been identified as one of the top 10 value-added potential platform chemicals from biomass, due to the variety of high-value chemicals that can be synthesized from it [2].

HMF is generally obtained through the dehydration of hexose sugars (mainly fructose) [3]. Various catalysts have been developed for the high conversion efficiency of fructose into HMF. Some homogeneous acid catalysts, such as sulfuric acids [4], hydrochloric acids [5], and phosphoric acids [6], exhibit high catalytic performance for the fructose-to-HMF transformation. However, there are some shortcomings in using these homogeneous acid catalysts, such as their strong corrosiveness and environmental pollution. In contrast, solid acid catalysts are noncorrosive and cause less environmental pollution. Many works have tried to develop heterogeneous acid catalysts for converting fructose to HMF, such as metal oxides [7], cation exchange resins [8], and zeolites [9]. Although significant achievements have been obtained, these catalysts have several drawbacks, including a tiny specific surface area (e.g., resin, S_{BET} 50 m²/g), an immobile pore structure, poor solubility of heteropoly acids (such as H₃PW₁₂O₄₀ [10]) in DMSO, and a low surface area (e.g., metal oxide catalysts). As a result, developing a novel heterogeneous catalyst for fructose dehydration is imperative.

In recent years, supported sulfonic acid ($-\text{SO}_3\text{H}$) catalysts have received much interest due to their remarkable performance in the fructose-to-HMF conversion [9,11,12]. Chen et al. [13] used $\text{NH}_2\text{SO}_3\text{H}$ as a catalyst in the conversion of dehydrated fructose to HMF and obtained a 94.3% yield at 110 °C. According to Morales et al. [14], employing the sulfonic commercial resin Amberlyst-70 as a catalyst resulted in a 93% HMF yield from fructose at 147 °C after 1 h. Wei et al. [15] used $\text{Fe}_3\text{O}_4@\text{SiO}_2\text{-SO}_3\text{H}$ as a catalyst for fructose dehydration and obtained a 96.1% yield of HMF.

SBA-15 is a mesoporous silica characterized by hexagonally ordered, cylindrical pores [11]. Its high surface area, well-defined porosity architecture, and capacity to incorporate metal atoms within the mesopores make it an attractive support material for developing a variety of different catalysts [16]. To date, many SBA-15-based catalysts have been developed, including SBA-15-supported zirconium [17], bifunctionalized sulfonated Zn-SBA-15 [18], TiO_2 -coated SBA-15 [19], cobalt-substituted SBA-15, and alanine-functionalized mesoporous SBA-15 [20]. Presently, functionalized SBA-15 has been successfully used in organic synthesis for C-C coupling reactions [21] and oxidation [22], as well as in other fields, such as adsorption [23] and drug delivery [24]. We anticipate that a sulfonic-acid-functionalized SBA-15 catalyst based on mesoporous SBA-15 with an increased mass transport diffusion and $-\text{SO}_3\text{H}$ group with Brønsted acidity would demonstrate high catalytic performance for synthesizing HMF from fructose dehydration.

This work used a post-treatment approach to prepare a sulfonic-acid-functionalized mesoporous SBA-15 catalyst (SBA-15- SO_3H) for fructose dehydration. SBA-15- SO_3H was characterized with FTIR, TEM, N_2 adsorption–desorption, and pyridine-FTIR. We discussed the effect of various reaction conditions, such as the reaction temperature and reaction time. Furthermore, the kinetics of fructose transformation with or without SBA-15- SO_3H catalysts were also investigated.

2. Experimental Section

2.1. Chemicals

P123 ($\text{EO}_{20}\text{PO}_{70}\text{EO}_{20}$), HCl (36%–38%), tetraethyl orthosilicate ($\text{SiO}_2 \geq 28.4\%$), dimethyl sulfoxide (DMSO, 99.5%), HMF (97%, Damas-beta), and dichloromethane ($\geq 99.5\%$) were purchased from Shanghai Titan Scientific Co., Ltd, Shanghai, China. Fructose (98–102%) was purchased from the Sinopharm Chemical Reagent Co., Ltd, Shanghai, China. Chlorosulfonic acid (99.0%) was purchased from Energy Chemical Co., Ltd, Shanghai, China. All chemicals were used as supplied without any further purification. Deionized water used in this work was prepared using a water purification system (Heal Force, Shanghai Shengke Equipment Co., Ltd., Shanghai, China).

2.2. Preparation of Sulfonic-Acid-Functionalized SBA-15 Catalyst

Original pure silica SBA-15 was synthesized according to Zhao et al. [11]. Briefly, P123 (4.0 g) was dissolved in deionized water (30 mL) and HCl (2 mol/L, 120 g) solution under sufficient stirring. After P123 was completely dissolved, TEOS (8.34 g) was added dropwise in a single step. The mixtures were continuously stirred at 40 °C for 6 h and crystallized in a Teflon-lined hydrothermal at 100 °C. After being filtered, washed, dried at 100 °C overnight, and calcined at 550 °C for 6 h, the pure silica SBA-15 sample was obtained as a white solid.

The synthesis of sulfonic-acid-functionalized SBA-15 was performed according to the previous literature [25]. Typically, 1 g SBA-15 is dispersed in 30 mL of dichloromethane in a three-necked flask equipped with a constant-pressure dropping funnel and stirred for 6 h. In total, 0.6 mL of chlorosulfonic acid was added dropwise into the above mixture for over 30 min in an ice bath. Afterward, the mixture was stirred for 2 h, after which the dichloromethane was removed and washed with ethanol. The obtained SBA-15- SO_3H catalyst was dried at 60 °C for 12 h. The obtained solid was named SBA-15- SO_3H .

2.3. Catalyst Characterization

FT-IR spectra were obtained on a Fourier transform infrared spectrometer (Nicolet-iS10, Thermo Scientific, Waltham, MA, USA) in the frequency range of 400–4000 cm^{-1} . The catalyst morphology was studied using transmission electron microscopy (TEM, Thermo Fisher Talos F200X, Waltham, MA, USA). The catalysts' specific surface areas (Brunauer–Emmett–Teller) were obtained using nitrogen adsorption–desorption measurements on a Micro for TriStar II Plus 2.02 instrument (Atlanta, GA, USA) at $-196\text{ }^\circ\text{C}$, and the mean pore sizes and pore volumes were determined using the Barrett–Joyner–Halenda method. Before the measurements, the samples were heated in a vacuum at $120\text{ }^\circ\text{C}$ for 6 h to eliminate moisture and volatile contaminants. A PerkinElmer Frontier FT-IR spectrometer was used to acquire pyridine-IR data with 64 scans at an effective resolution of 1 cm^{-1} . A 10 mg sample was squeezed into a wafer that could stand independently. Prior to adsorption, the materials were processed at $350\text{ }^\circ\text{C}$ under vacuum and then cooled to ambient temperature before pyridine vapor was added into the cell. The samples were heated in a vacuum to $150\text{ }^\circ\text{C}$, and the spectra were taken at room temperature. Elemental analysis of S-element content was qualitatively determined with Elementar Vario Micro Cube (Elementar, Langensfeld, Germany).

2.4. Catalytic Performance

In a typical catalytic reaction, 0.1 g of fructose and the 0.05 g catalyst are mixed with 10 mL of DMSO in a 15 mL pressure tube with magnetic stirring. Using an oil bath, the reactor was heated to the necessary reaction temperature, stirring at 500 rpm. The tube was taken out of the oil bath after a certain period, cooled to room temperature, and then the liquid reaction mixture was passed through a $0.45\text{ }\mu\text{m}$ filter before analysis.

The HMF yield was determined using a CoMetro 6000 HPLC system (Rheodyne, Cotati, CA, USA) with an ultraviolet-visible detector. A Waters C18 column ($250\text{ mm} \times 4.6\text{ mm}$, $5\text{ }\mu\text{m}$) was used for chromatographic separation. A mobile phase of water and methanol (90:10, v/v) was used for the isocratic elution. The column temperature, flow rate, and injection volume were maintained at $30\text{ }^\circ\text{C}$, 0.6 mL/min , and $20\text{ }\mu\text{L}$, respectively. A Shimadzu liquid chromatography system with a refractive index detector (RID-20A) measured fructose conversion using a COSMOSIL packed column of D-sugars ($250\text{ mm} \times 4.6\text{ mm}$) at $30\text{ }^\circ\text{C}$ with a flow rate of 1 mL/min and a mobile phase of acetonitrile and water (75:25, v/v).

The yield of HMF and the conversion of fructose were calculated using the external standard and are defined as follows:

$$\text{Conversion (fructose, \%)} = \left(1 - \frac{\text{mols of remaining fructose}}{\text{Initial mols of fructose}}\right) \quad (1)$$

$$\text{Yield of HMF(\%)} = \frac{\text{mols of HMF}}{\text{Initial mols of fructose}} \times 100 \quad (2)$$

3. Results and Discussion

3.1. Catalyst Characterization

Figure 1 illustrates the N_2 adsorption-desorption isotherms of the sulfonic-acid-functionalized SBA-15. The SBA-15 and SBA-15- SO_3H exhibited a type IV adsorption isotherm, indicating the existence of a mesoporous material, consistent with the TEM results. All isotherms had a sharp condensation step at relative pressure in the range of 0.6–0.8. However, the SBA-15- SO_3H samples had smaller hysteresis loops and narrower channels than the SBA-15 samples, which also had a mesoporous feature. Information about the BET surface area, pore volume, and pore size of SBA-15- SO_3H is summarized in Table 1. Compared with pure SBA-15 ($868\text{ m}^2/\text{g}$), the BET surface area of sulfonic-acid-functionalized SBA-15 was reduced to $200\text{ m}^2/\text{g}$. The two samples' pore sizes and pore volumes ranged from 5.96 to 9.96 nm and from 1.29 to $0.48\text{ cm}^3/\text{g}$, respectively. This was due to the inclusion of SO_3H in the SBA-15 framework (as shown in Table 1). As a consequence of acid treatment, the sample became more porous, and the mesopore size

increased significantly [26]. Therefore, the BET surface area decreased, the average pore size increased, and the pore volume decreased. This indicated the successful grafting of $-SO_3H$ onto SBA-15. The ICP-OES measurement was carried out to analyze the catalyst's elements, and the S-element content was 9.08 wt%.

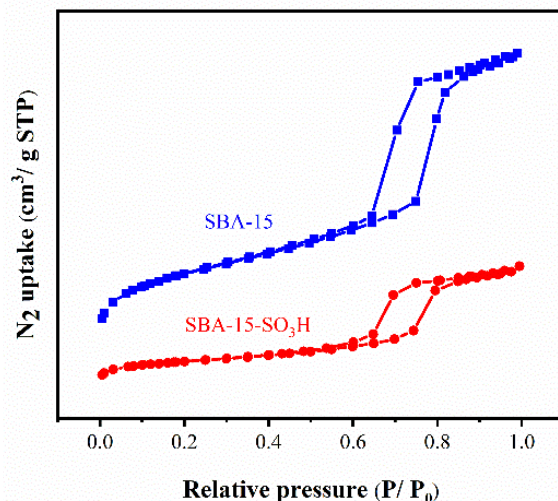


Figure 1. N_2 adsorption–desorption isotherms of SBA-15- SO_3H catalysts.

Table 1. Characterization of SBA-15 and SBA-15- SO_3H .

Catalyst	BET Surface Area ($m^2 g^{-1}$) ¹	Pore Volume ($cm^3 g^{-1}$) ¹	Pore Size (nm) ¹	S-Element Content (wt%) ²	L (mmol $Py \cdot g^{-1}$) ³	B (mmol $Py \cdot g^{-1}$) ³
SBA-15	868	1.29	5.96	/	/	/
SBA-15- SO_3H	200	0.48	9.66	9.08	0	0.34

¹ Surface area, pore volume, and pore size were measured with N_2 adsorption–desorption. ² S-element content was determined with elemental analysis. ³ L and B acid contents were determined with pyridine-IR.

Figure 2 shows TEM images of SBA-15- SO_3H . The produced SBA-15- SO_3H sample retained well-ordered hexagonal arrays of mesopores connected by one-dimensional channels, indicating a two-dimensional hexagonal ($p6mm$) mesostructure. Depending on the transmission electron microscopy, the introduction of the sulfonic acid group may have fractured the mesoporous structure to varying extents. However, the mesoporous structure was clearly observed.

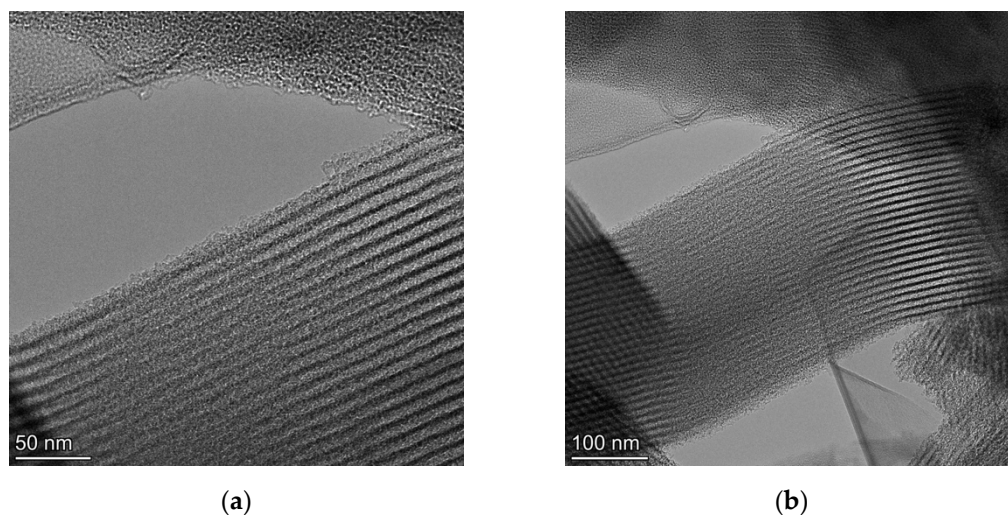


Figure 2. TEM images of SBA-15- SO_3H with (a) 50 nm and (b) 100 nm.

The SBA-15 and SBA-15-SO₃H chemical structures were characterized with FT-IR analysis (Figure 3). Both spectra showed bands at 3425 cm⁻¹ that could be assigned to the O-H stretching vibration, while the absorbances at 1089 cm⁻¹ and 807 cm⁻¹ were attributed to the Si-O stretching vibration. The 463 cm⁻¹ band originated from the bending vibration of the Si-O-Si groups. For SBA-15-SO₃H, a band at approximately 574 cm⁻¹ was attributed to the S-O stretching vibration. A band at approximately 3450 cm⁻¹, which is typically assigned to the -O-H stretching vibration of sulfonic groups, was observed [25]. The peak at approximately 1169 cm⁻¹ was attributed to the O=S=O stretching vibration, demonstrating that the SO₃H groups were successfully bonded after SBA-15 was treated with chlorosulfonic acid, in accordance with the elemental analysis results (Table 1).

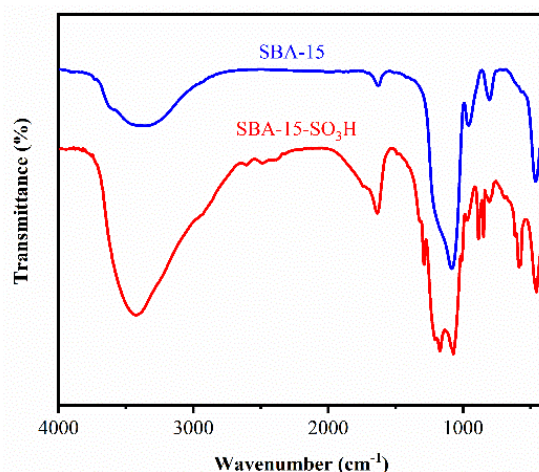


Figure 3. FTIR of SBA-15 and SBA-15-SO₃H catalysts.

Additionally, pyridine FT-IR was employed to determine acidic properties of SBA-15-SO₃H (Figure 4). In the SBA-15-SO₃H sample, the distinctive bands at 1544 cm⁻¹ corresponded to pyridine attached to strong Brønsted acid sites, revealing that the as-prepared materials contained Brønsted acid sites. Furthermore, the results indicated that the produced SBA-15-SO₃H catalyst did not contain any Lewis acid sites, represented as the absence of characteristic absorption peaks at 1450 cm⁻¹. This was consistent with the findings in Table 1, columns 6–7. The Brønsted acid amount was 0.34 mmol/g. A peak at 1489 cm⁻¹, attributable to both Lewis and Brønsted acid sites, was also observed. Altogether, the results demonstrated that -SO₃H was successfully grafted on the SBA-15 support.

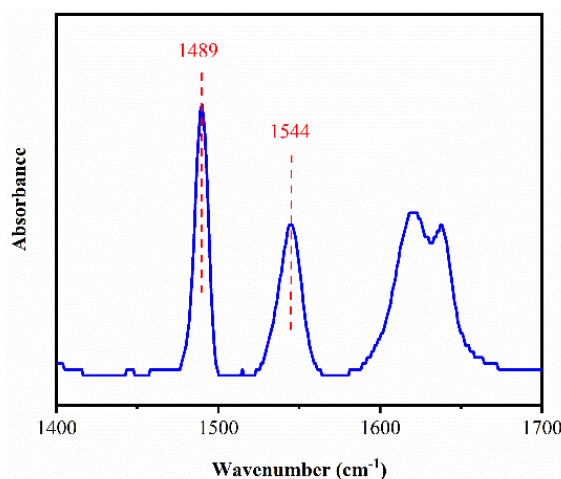


Figure 4. Pyridine-FTIR spectra of SBA-15-SO₃H samples collected after treatment at 150 °C under vacuum.

3.2. Catalyst Activity

To demonstrate the effect of the reaction temperature and time on the fructose-to-HMF conversion, the reaction was conducted without any catalysts (blank sample) and with a SBA-15-SO₃H catalyst, respectively. Sixteen reaction temperatures in the range of 20 to 170 °C were examined to evaluate the temperature effect on the transformation, and to determine the effect of the SBA-15-SO₃H catalyst on the fructose-to-HMF conversion. These temperatures (20–170 °C) were chosen as we wanted to have a temperature near ambient conditions to minimize the energy required and the occurrence of side reactions. The reaction temperature strongly impacted the fructose-to-5-HMF conversion, and the results are shown in Figure 5. In the cases of blank experiments (no catalyst), no HMF was yielded at 100 °C, indicating that the dehydration of fructose to HMF without any catalyst was difficult at 100 °C. In contrast, under the same reaction conditions, the reaction proceeded in the presence of SBA-15-SO₃H, surprisingly exhibiting an enhanced HMF yield, as high as 68% at 100 °C. The results showed that SBA-15-SO₃H could act rapidly (40 °C, 1 h) to promote a hydrolysis reaction at low temperatures. Therefore, SBA-15-SO₃H catalysts improved the reaction rate of the catalytic production of HMF. As a result of higher temperatures and a long reaction time, humins and carboxylic acid degradation products were formed, preventing the production of HMF [27]. Therefore, in noncatalyzed reactions, 140 °C led to decreased HMF yields, whereas in catalyzed reactions, 120 °C led to decreased yields.

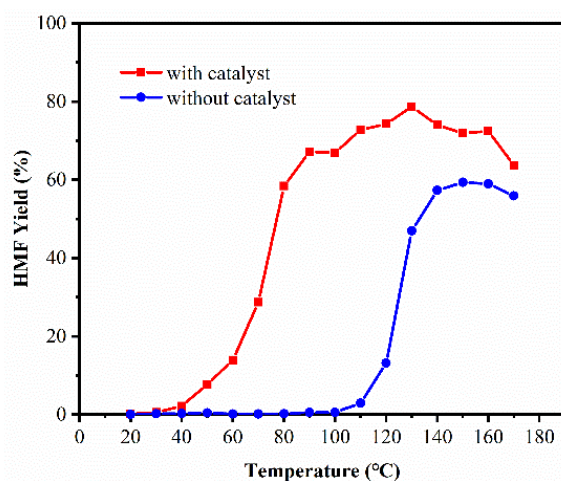


Figure 5. Effect of reaction temperature on fructose-to-HMF conversion with and without SBA-15-SO₃H (reaction conditions: 0.1 g fructose, 0.05 g SBA-15-SO₃H, 20–170 °C, 10 mL DMSO, 1 h).

Figure 6 displays the fructose conversion and 5-HMF yields at different temperatures with SBA-15-SO₃H or without any catalyst. As shown in Figure 6a,b, the conversion of fructose in the presence of SBA-15-SO₃H was substantially higher than without SBA-15-SO₃H, confirming the significant catalytic effect of SBA-15-SO₃H. A lower temperature favored the fructose conversion, and fructose was almost completely converted at 60 °C within 1 h through SBA-15-SO₃H catalysis. At a higher temperature (80 °C, 100 °C, and 120 °C), the reactions decreased the HMF yield with increasing reaction time (Figure 6c,d). This suggested that the reactants already ran out, resulting in no more HMF being produced. The most important factor causing the decline in the HMF yield in nonaqueous media is HMF's self-polymerization or cross-polymerization with fructose, followed by polymerization to humins [12,28]. It is noteworthy that a higher temperature does not always favor yielding 5-HMF. However, the addition of the as-synthesized catalyst, SBA-15-SO₃H, accelerated HMF generation to some extent. A lower temperature (e.g., 60 °C and 80 °C) did not favor fructose conversion; almost no HMF was observed without SBA-15-SO₃H. At the same temperature (60 °C and 80 °C), a large amount of HMF was produced with SBA-15-SO₃H. At low reaction temperatures, SBA-15-SO₃H could also be active in fructose dehydration

to HMF. In the absence of a catalyst, no HMF was formed under 100 °C within the first 5 h. Theoretical research demonstrated that when a Brønsted acid is present, H^+ prefers to interact with DMSO to generate the $[DMSOH]^+$ active species, which has catalytic activity in removing three H_2O molecules from fructose [29,30].

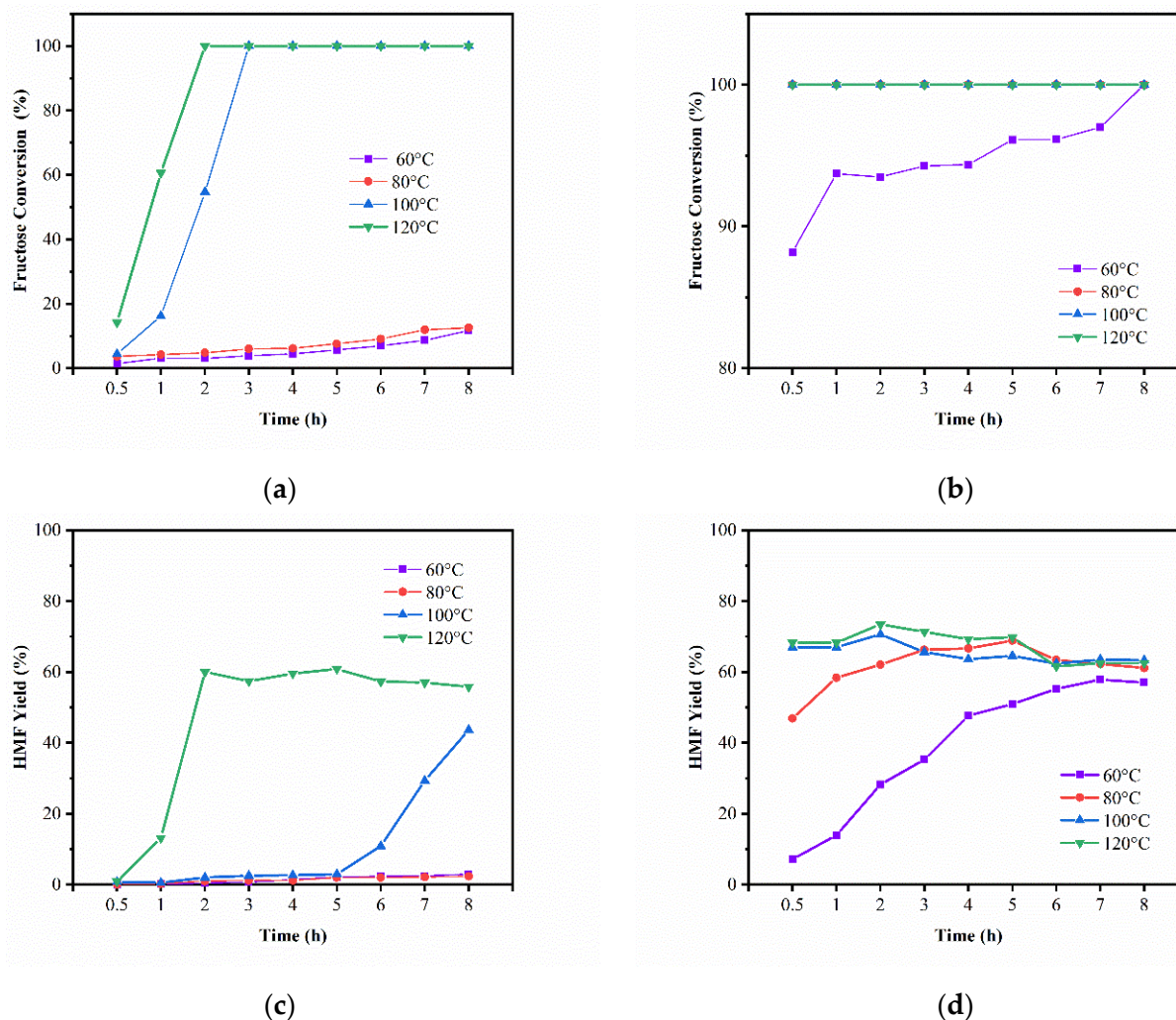


Figure 6. (a) Effect of reaction temperature and time on fructose conversion without catalysts; (b) effect of reaction temperature and time on fructose conversion with SBA-15-SO₃H; (c) effect of reaction temperature and time on HMF yield without catalysts; (d) effect of reaction temperature and time on HMF yield with SBA-15-SO₃H (reaction conditions: 0.1 g fructose, 0.05 g SBA-15-SO₃H, 10 mL DMSO).

There are two possible reasons why fructose was also hydrolyzed to HMF in DMSO (above the 100 °C) without catalysts. On the one hand, utilizing DMSO as a solvent lowers the water concentration in the reaction system, preventing HMF rehydration or humin production. On the other hand, the furanoid form of fructose, which dehydrates rapidly to HMF, is favored in DMSO due to its strong polarity. In general, there was only a little HMF product appearing at the early stages (60 °C) with and/or without the catalyst at low temperatures (below 120 °C). In other words, our catalysts took effect in the catalytic fructose conversion.

3.3. Comparison of the Activity with Other Reported Catalysts

Many different Brønsted acid catalysts have been described to produce HMF from fructose in DMSO. Among the most prevalent of Brønsted catalysts, SBA-15-SO₃H proved superior. For example, Lee et al. [31] used mesoporous silica nanoparticles functionalized

with both sulfonic acid (HSO_3) and ionic liquids (ILs) in DMSO (at $90\text{ }^\circ\text{C}$, 1h), and the HMF yield was close to 35% (Table 2, line 5), while, in our system, the reaction temperature was $80\text{ }^\circ\text{C}$ for 1 h, resulting in a yield of 59% HMF. Table 2 shows that by utilizing DMSO as a solvent and at high temperatures of $140\text{ }^\circ\text{C}$, a highly sulfonated polyaniline-based organocatalyst (S-A-PAN-H) achieved an 88.8% yield of HMF from fructose. Nevertheless, this result was obtained under an atmosphere of nitrogen. SBA-15- SO_3H could provide HMF in a 74% yield ($140\text{ }^\circ\text{C}$, 1h) without N_2 , compared with the yield obtained by using the S-A-PAN-H catalytic system. However, a N_2 atmosphere is very costly and tedious, and it is not suitable for the large-scale production of HMF [32]. Li et al. [33] demonstrated that sulfonated graphene quantum dots (SGQDs) could degrade fructose with an HMF yield of 51.7% after 2 h at $170\text{ }^\circ\text{C}$. In our system, a higher HMF yield (63.6%) at the same temperature was achieved within 1 h. Similarly, N-methyl-2-pyrrolidonium hydrogen sulfate ($[\text{NMP}]^+ [\text{HSO}_4]^-$) showed a 69.4% HMF yield and 70.4% selectivity at $90\text{ }^\circ\text{C}$ after 2 h. Nevertheless, a higher HMF yield (67.2%) was obtained at a shorter reaction time (1 h) for the same reaction temperature, which was insignificantly different from $[\text{NMP}]^+ [\text{HSO}_4]^-$ [34]. Good selectivity was obtained using H_2SO_4 [35]. However, the inherent disadvantages of H_2SO_4 , such as high corrosivity and difficulties in separation, limit its practical applications. Similarly, the homogeneous catalyst acid poly (4-styrenesulfonic acid) (PSS) was obtained in a good HMF yield. However, it can pollute the environment, so it is not recommended for practical applications. Additionally, the efficacies of SBA-15- SO_3H catalysts on the fructose conversion to HMF in a DMSO solvent were studied at $130\text{ }^\circ\text{C}$ for 1 h. In the absence of a catalyst, a small amount of HMF (46.9%) was formed, indicating fructose conversion in the absence of catalysts was difficult. The yield of 5-HMF was small when unmodified SBA-15 was employed, suggesting that SBA-15 had no effect on the conversion of fructose. The above results implied that the SBA-15- SO_3H catalyst hydrolysis reaction was relatively facile, with mild reaction conditions, short reaction times, environment protection, and high yields of the products.

Table 2. Current advances in fructose-to-HMF conversion by using Brønsted acid catalysts in DMSO.

Entry	Catalysts	Reaction Condition		Catalyst Activity		Ref.
		Temp ($^\circ\text{C}$)	Time (h)	Yield (%)	Selectivity (%)	
1	($\text{HSO}_3 + \text{CP}$)-MSN	90	1	35	/	[31]
2	S-A-PAN-H	140	0.75	88.8	89	[32]
3	SGQDs	170	2	51.7	56.3	[33]
4	$[\text{NMP}]^+ [\text{HSO}_4]^-$	90	2	69.4	70.4	[34]
5	H_2SO_4	150	0.5	/	84	[35]
6	PSS	130	6	48.5	/	[36]
7	SBA-15- SO_3H	80	1	58.4	/	This work
8	SBA-15- SO_3H	130	1	78.7	/	This work
9	Without catalysts	130	1	46.9	/	This work
10	SBA-15	130	1	45.6	/	This work

3.4. Kinetic Studies

To obtain more insight into the hydrolysis reaction of fructose over SBA-15- SO_3H , we further studied the fructose-to-HMF conversion kinetics and compared the rate constants and activation energies for systems with SBA-15- SO_3H and without any catalyst (Figure 7). For the purpose of identifying the relationships between kinetic parameters (such as rate constants, reaction orders, and activation energies) and the addition of a sulfonic-acid-functionalized catalyst, we further comprehensively constructed kinetic profiles at different temperatures for systems without catalysts and with SBA-15- SO_3H . Based on the reaction pathways, a kinetic model was developed for fructose conversion. To develop the model, the following assumptions were determined:

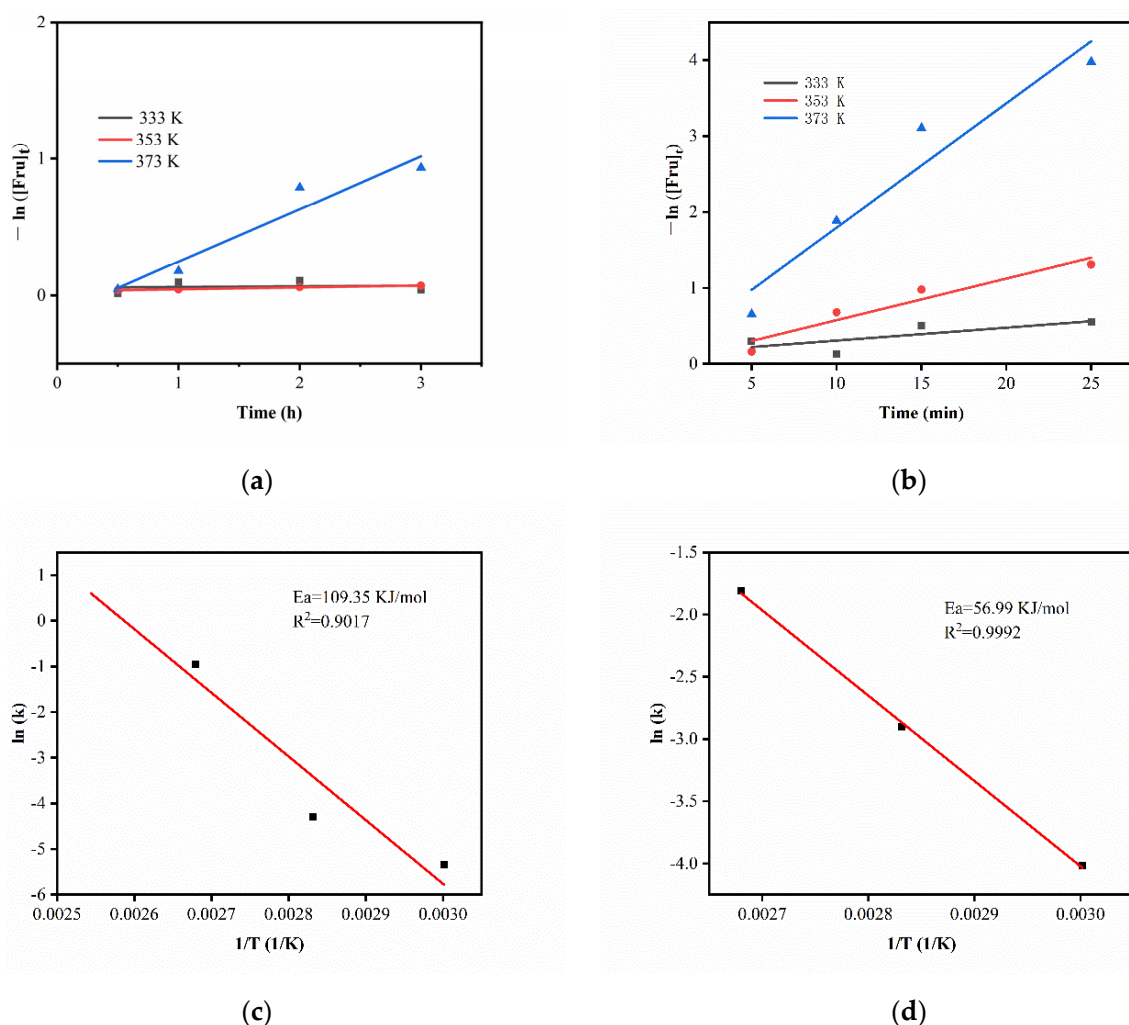


Figure 7. (a) Kinetic profiles of fructose-to-HMF conversion without catalysts; (b) kinetic profiles of fructose-to-HMF conversion over SBA-15-SO₃H; (c) Arrhenius plot of the formation of HMF from fructose without catalysts; (d) Arrhenius plot of the formation of HMF from fructose.

- (i) There were no reversible reactions and they were all pseudo-first-order reactions.
- (ii) The main decomposition product of fructose was HMF. Other probable reactions were insignificant.
- (iii) Humins and other polymeric compounds were assumed to be byproducts.
- (iv) All other intermediates had negligible concentrations.

In addition to this, we hypothesized that HMF degradation would not exist under our designed conditions (60–100 °C, 5 min–3 h). We examined the kinetic data to systematically determine the shifts of each kinetic rate parameter caused by SBA-15-SO₃H, as shown in Figure 7. A first-order kinetics model was assumed [37]. The reaction rate equation could be shown as follows:

$$k[fru] = \frac{d[fru]}{dt} \quad (3)$$

where $[fru]$ = molar concentration of fructose and k = the rate constant for fructose conversion at a certain temperature. Next, we transformed this equation into a numerical form and determined $[fructose]_t$ in terms of conversion X , i.e., $[fructose]_t = [fructose]_{t_0} (1 - X)$. After subsequent integral research and calculations, the force parameter expression of original equation would become:

$$-\ln(1 - X) = kt + C \quad (4)$$

where t = the reaction time specified in hours and C = an arbitrary constant. Results were plotted with $-\ln(1 - X)$ on the Y-axis against the time on the X-axis (Figure 7). We fitted the data linearly and computed the reaction constants from the slopes of the linear approximations. An obvious increase in K was observed for systems with SBA-15-SO₃H, confirming the ability of SBA-15-SO₃H to promote fructose hydrolysis.

It was visually observed that the reaction rate constant increased with the increase in reaction temperature, clearly indicating that a high reaction temperature was conducive to promoting the hydrolysis reaction of fructose in Figure 7. This deduction was further confirmed by the fact that the formation of HMF rate increased with increasing reaction temperature, which, in turn, could not be too high, according to previous conclusions.

The calculated activation energy (E_a) of systems without catalysts and with SBA-15-SO₃H are shown in Table 3. The apparent E_a was obtained by fitting the results with the Arrhenius equation. As a result, the E_a of systems with and without SBA-15-SO₃H was 56.99 and 109.35 kJ/mol, respectively. This finding revealed that SBA-15-SO₃H altered the reaction pathway to some extent, lowering the E_a and resulting in a greater reaction rate. This finding agreed with the earlier result in Figure 7.

Table 3. Rate constants and reaction activation energy for fructose dehydration with and without catalysts.

	Temperature (°C)	K	E_a (kJ/mol)	R^2
With catalysts	60	0.018	56.99	0.9992
	80	0.0548		
	100	0.1637		
Without catalysts	60	0.0048	109.35	0.9017
	80	0.0137		
	100	0.346		

4. Conclusions

This study offered a preliminary finding on the possibility of sulfonic-acid-functionalized SBA-15 (SBA-15-SO₃H) as a highly active catalyst for the conversion of fructose to HMF. The -SO₃H groups served as catalytically active sites, facilitating fructose dehydration with a 78.7% yield of HMF after 1 h at 130 °C. Several parameters (reaction time and temperature) were evaluated to determine the catalytic system with and without an SBA-15-SO₃H catalyst. Such sulfonic-acid-functionalized SBA-15 solid catalysts enhanced the yield of HMF from fructose dehydration under mild conditions using DMSO as the solvent. A kinetics study showed that our SBA-15-SO₃H could accelerate fructose dehydration by reducing the activation energy. We considered this an essential step towards the sustainable, green processing of biomass in the future. It is expected that the SBA-15-SO₃H solid catalyst can also be used in other catalytic processes.

Author Contributions: Writing—original draft preparation, Y.Z.; writing—review and editing, X.X.; writing—review and editing, J.H.; writing—review and editing, J.G.; writing—review and editing, K.S. All authors have read and agreed to the published version of the manuscript.

Funding: This research was funded by the Key Project of Hunan Provincial Education Department (grant number 20A412).

Data Availability Statement: The data presented in this study are available on request from the corresponding author. The data are not publicly available.

Conflicts of Interest: The authors declare no conflict of interest.

References

1. Davidson, M.G.; Elgie, S.; Parsons, S.; Young, T.J. Production of HMF, FDCA and their derived products: A review of life cycle assessment (LCA) and techno-economic analysis (TEA) studies. *Green Chem.* **2021**, *23*, 3154–3171. [[CrossRef](#)]
2. Qiu, G.; Huang, C.; Sun, X.; Chen, B. Highly active niobium-loaded montmorillonite catalysts for the production of 5-hydroxymethylfurfural from glucose. *Green Chem.* **2019**, *21*, 3930–3939. [[CrossRef](#)]
3. Nunes, R.S.; Reis, G.M.; Vieira, L.M.; Mandelli, D.; Carvalho, W.A. Ultra-fast selective fructose dehydration promoted by a kraft lignin sulfonated carbon under microwave heating. *Catal. Lett.* **2021**, *151*, 398–408. [[CrossRef](#)]
4. Antal Jr, M.J.; Mok, W.S.; Richards, G.N. Mechanism of formation of 5-(hydroxymethyl)-2-furaldehyde from D-fructose and sucrose. *Carbohydr. Res.* **1990**, *199*, 91–109. [[CrossRef](#)]
5. Román-Leshkov, Y.; Chheda, J.N.; Dumesic, J.A. Production of hydroxymethylfurfural from fructose in a biphasic system using aqueous- and organic- phase modifiers. *Science* **2006**, *312*, 1933–1937. [[CrossRef](#)]
6. Asghari, F.S.; Yoshida, H. Acid-catalyzed production of 5-hydroxymethyl furfural from D-fructose in subcritical water. *Ind. Eng. Chem. Res.* **2006**, *45*, 2163–2173. [[CrossRef](#)]
7. Qi, X.H.; Guo, H.X.; Li, L.Y. Efficient conversion of fructose to 5-hydroxymethylfurfural catalyzed by sulfated zirconia in ionic liquids. *Ind. Eng. Chem. Res.* **2011**, *50*, 7985–7989. [[CrossRef](#)]
8. Qi, X.H.; Watanabe, M.; Aida, T.M.; Smith, R.L., Jr. Efficient catalytic conversion of fructose into 5-hydroxymethylfurfural in ionic liquids at room temperature. *Chem. Sustain. Energy Mater.* **2009**, *2*, 944–946. [[CrossRef](#)] [[PubMed](#)]
9. Sun, S.; Zhao, L.J.; Yang, J.R.; Wang, X.Q.; Qin, X.Y.; Qi, X.H.; Shen, F. Eco-friendly synthesis of SO₃H-containing solid acid via mechanochemistry for the conversion of carbohydrates to 5-hydroxymethylfurfural. *ACS Sustain. Chem. Eng.* **2020**, *8*, 7059–7067. [[CrossRef](#)]
10. Gomes, F.; Mendes, F.; Souza, M. Synthesis of 5-hydroxymethylfurfural from fructose catalyzed by phosphotungstic acid. *Catal. Today* **2017**, *279*, 296–304. [[CrossRef](#)]
11. Zhao, D.Y.; Feng, J.L.; Huo, Q.S.; Melosh, N.; Fredrickson, G.H.; Chmelka, B.F.; Stucky, G.D. Triblock Copolymer Syntheses of Mesoporous Silica with Periodic 50 to 300 Angstrom Pores. *Science* **1998**, *279*, 548–552. [[CrossRef](#)] [[PubMed](#)]
12. Li, K.; Du, M.; Ji, P.J. Multifunctional tin-based heterogeneous catalyst for catalytic conversion of glucose to 5-hydroxymethylfurfural. *ACS Sustain. Chem. Eng.* **2018**, *6*, 5636–5644. [[CrossRef](#)]
13. Chen, G.Z.; Sun, Q.H.; Xu, J.; Zheng, L.F.; Rong, J.F.; Zong, B.N. Sulfonic Derivatives as Recyclable Acid Catalysts in the Dehydration of Fructose to 5-Hydroxymethylfurfural in Biphasic Solvent Systems. *ACS Omega* **2021**, *6*, 6798–6809. [[CrossRef](#)] [[PubMed](#)]
14. Morales, G.; Melero, J.A.; Paniagua, M.; Iglesias, J.; Hernández, B.; Sanz, M. Sulfonic acid heterogeneous catalysts for dehydration of C₆-monosaccharides to 5-hydroxymethylfurfural in dimethyl sulfoxide. *Chin. J. Catal.* **2014**, *35*, 644–655. [[CrossRef](#)]
15. Wei, W.Q.; Lyu, G.J.; Jiang, W.K.; Chen, Z.Y.; Wu, S.B. High-efficiency synthesis of 5-hydroxymethylfurfural and 2, 5-diformylfuran from fructose over magnetic separable catalysts. *J. Colloid Interf. Sci.* **2021**, *602*, 146–158. [[CrossRef](#)]
16. Verma, P.; Kuwahara, Y.; Mori, K.; Raja, R.; Yamashita, H. Functionalized mesoporous SBA-15 silica: Recent trends and catalytic applications. *Nanoscale* **2020**, *12*, 11333–11363. [[CrossRef](#)]
17. Xu, W.; Yu, B.; Zhang, Y.; Chen, X.; Zhang, G.F.; Gao, Z.W. Single-site SBA-15 supported zirconium catalysts. Synthesis, characterization and toward cyanosilylation reaction. *Appl. Surf. Sci.* **2015**, *325*, 227–234. [[CrossRef](#)]
18. Zhang, J.H.; Cheng, K.; Li, H.Y.; Yin, F.W.; Wang, Q.; Cui, L.; Yang, S.S.; Nie, J.G.; Zhou, D.Y.; Zhu, B.W. Efficient Synthesis of Structured Phospholipids Containing Short-Chain Fatty Acids over a Sulfonated Zn-SBA-15 Catalyst. *J. Agric. Food Chem.* **2020**, *8*, 12444–12453. [[CrossRef](#)]
19. Héroguel, F.; Silvioli, L.; Du, Y.P.; Luterbacher, J.S. Controlled deposition of titanium oxide overcoats by non-hydrolytic sol gel for improved catalyst selectivity and stability. *J. Catal.* **2018**, *358*, 50–61. [[CrossRef](#)]
20. Appaturi, J.N.; Pulingam, T.; Rajabathar, J.R.; Khoerunnisa, F.; Ling, T.C.; Tan, S.h.; Ng, E. Acid-base bifunctional SBA-15 as an active and selective catalyst for synthesis of ethyl α -cyanocinnamate via Knoevenagel condensation. *Microporous Mesoporous Mater.* **2021**, *320*, 111091–111101. [[CrossRef](#)]
21. Joseph, T.; Deshpande, S.S.; Halligudi, S.B.; Vinu, A.; Ernst, S.; Hartmann, M. Hydrogenation of olefins over hydrido chloro-carbonyl tris-(triphenylphosphine) ruthenium (II) complex immobilized on functionalized MCM-41 and SBA-15. *J. Mol. Catal. A-Chem.* **2003**, *206*, 13–21. [[CrossRef](#)]
22. Suib, S.L.; Přeč, J.; Čejka, J.; Kuwahara, Y.; Mori, K.; Yamashita, H. Some novel porous materials for selective catalytic oxidations. *Mater. Today* **2020**, *32*, 244–259. [[CrossRef](#)]
23. Gatti, G.; Costenaro, D.; Vittoni, C.; Paul, G.; Crocellà, V.; Mangano, E.; Brandani, S.; Bordiga, S.; Cossi, M.; Marchese, L.; et al. CO₂ adsorption on different organo-modified SBA-15 silicas: A multidisciplinary study on the effects of basic surface groups. *Phys. Chem. Chem. Phys.* **2017**, *19*, 14114–14128. [[CrossRef](#)] [[PubMed](#)]
24. Vavsari, V.F.; Ziarani, G.M.; Badieli, A. The role of SBA-15 in drug delivery. *RSC Adv.* **2015**, *5*, 91686–91707. [[CrossRef](#)]
25. Xiang, Y.P.; Wen, S.; Tian, Y.; Zhao, K.Y.; Guo, D.W.; Cheng, F.; Xu, Q.; Liu, X.X.; Yin, D.L. Efficient synthesis of 5-ethoxymethylfurfural from biomass-derived 5-hydroxymethylfurfural over sulfonated organic polymer catalyst. *RSC Adv.* **2021**, *11*, 3585–3595. [[CrossRef](#)] [[PubMed](#)]

26. Huang, H.L.; Li, J.R.; Wang, K.K.; Han, T.T.; Tong, M.M.; Li, L.S.; Xie, Y.B.; Yang, Q.Y.; Liu, D.H.; Zhong, C.L. An in Situ Self-Assembly Template Strategy for The Preparation of Hierarchical-Pore Metal-Organic Frameworks. *Nat. Commun.* **2015**, *6*, 1–8. Available online: <https://www.nature.com/articles/ncomms9847> (accessed on 28 August 2022). [[CrossRef](#)] [[PubMed](#)]
27. Li, X.L.; Li, M.M.; Liu, Y.X.; Feng, Y.S.; Pan, P. Preparation of 5-hydroxymethylfurfural using magnetic Fe₃O₄@SiO₂@mSiO₂-TaOPO₄ catalyst in 2-pentanol. *Rsc. Adv.* **2022**, *12*, 13251–13260. [[CrossRef](#)] [[PubMed](#)]
28. Hao, J.W.; Mao, W.; Ye, G.R.; Xia, Y.; Wei, C.; Zeng, L.; Zhou, J.H. Tin–chromium bimetallic metal–organic framework MIL-101 (Cr, Sn) as a catalyst for glucose conversion into HMF. *Biomass Bioenergy* **2022**, *159*, 106395–106404. [[CrossRef](#)]
29. Hu, Y.; Li, M.; Gao, Z.; Wang, L.; Zhang, J. Leaf-derived sulfonated carbon dots: Efficient and recoverable catalysts to synthesize 5-hydroxymethylfurfural from fructose. *Mater. Today Chem.* **2021**, *20*, 100423–100430. [[CrossRef](#)]
30. Jing, Y.X.; Guo, Y.; Xia, Q.; Liu, X.H.; Wang, Y.Q. Catalytic Production of Value-Added Chemicals and Liquid Fuels from Lignocellulosic Biomass. *Chem* **2019**, *5*, 1–27. [[CrossRef](#)]
31. Lee, Y.Y.; Wu, C.W. Conversion and kinetics study of fructose-to-5-hydroxymethylfurfural (HMF) using sulfonic and ionic liquid groups bi-functionalized mesoporous silica nanoparticles as recyclable solid catalysts in DMSO systems. *Phys. Chem. Chem. Phys.* **2012**, *14*, 13914–13917. [[CrossRef](#)] [[PubMed](#)]
32. Liu, Z.B.; Zhu, L.F.; Hu, C.W. High-efficiency synthesis of 5-hydroxymethylfurfural from fructose over highly sulfonated organocatalyst. *Ind. Eng. Chem. Res.* **2020**, *59*, 17218–17227. [[CrossRef](#)]
33. Li, K.X.; Chen, J.; Yan, Y.B.; Min, Y.G.; Li, H.P.; Xi, F.N.; Liu, J.Y.; Chen, P. Quasi-homogeneous carbocatalysis for one-pot selective conversion of carbohydrates to 5-hydroxymethylfurfural using sulfonated graphene quantum dots. *Carbon* **2018**, *136*, 224–233. [[CrossRef](#)]
34. Tong, X.L.; Li, Y.D. Efficient and selective dehydration of fructose to 5-hydroxymethylfurfural catalyzed by Brønsted-acidic ionic liquids. *Chem. Sustain. Energy Mater.* **2010**, *3*, 350–355. [[CrossRef](#)] [[PubMed](#)]
35. Svenningsen, G.S.; Kumar, R.; Wyman, C.E.; Christopher, P. Unifying mechanistic analysis of factors controlling selectivity in fructose dehydration to 5-hydroxymethylfurfural by homogeneous acid catalysts in aprotic solvents. *ACS Catal.* **2018**, *8*, 5591–5600. [[CrossRef](#)]
36. Shi, S.B.; Wu, Y.F.; Liu, P.L.; Zhang, M.T.; Zhang, Z.Q.; Gao, L.J.; Xiao, G.M. Efficient conversion of carbohydrates to 5-hydroxymethylfurfural over poly(4-styrenesulfonic acid) catalyst. *Catal. Lett.* **2022**, *152*, 954–961. [[CrossRef](#)]
37. Wang, L.; Zhang, L.B.; Li, H.Y.; Ma, Y.B.; Zhang, R.H. High selective production of 5-hydroxymethylfurfural from fructose by sulfonic acid functionalized SBA-15 catalyst. *Compos. Part B-Eng.* **2019**, *156*, 88–94. [[CrossRef](#)]